Electronic Supplementary Material (ESI) for Journal of Materials Chemistry A.

Supporting Information

In-situ switchable nanofiber films based on photoselective asymmetric assembly towards year-round energy saving

Liuqian An[a], Jiaxiang Ma[a], Peizhi Wang[a], Jinxin Yao[a], Aleksandr Kuchmizha[c], Wei Wang[a], Hongbo Xu*[b]*

[a] State Key Laboratory of Urban Water Resource and Environment, School of Environment, Harbin Institute of Technology, Harbin 150090, Heilongjiang, China.

[b] MIIT Key Laboratory of Critical Materials Technology for New Energy Conversion and Storage, School of Chemistry and Chemical Engineering, Harbin Institute of Technology, 150001, Harbin, China.

[c] Institute of Automation and Control Processes, Far Eastern Branch, Russian Academy of Science, Vladivostok, Russia, Far Eastern Federal University, Vladivostok, Russia.

1. Building the scattering model

Chandrasekhar's radiative transfer formula was used to investigate the scattering of the PSP film-switching process

$$R_{sca}(\lambda) = \frac{\frac{3}{4}\rho\sigma_{sca}(\lambda)t}{1+\frac{3}{4}\rho\sigma_{sca}(\lambda)t} \qquad \text{(Equation 1)}$$

Where λ is the wavelength of the incident light, ρ is the porosity density of the film, $\sigma_{sca}(\lambda)$ is the spectral scattering cross section of a single nanopore, which calculated by Mie scattering solver, t is the thickness of the film.

2. PSP film heat energy analysis

The thermal balance of the system is influenced by the material's photothermal conversion capabilities as well as heat radiation from the environment. At the same time, temperature convection and heat conduction will cause some heat loss, as shown in Figure. S4. Equation1 depicts the particular thermal balance.

$$P_{net} = P_{sun} + P_{atm}(T_{amb}) - P_{cond + conv}(T,T_{amb}) \qquad \text{(Equation 2)}$$

P_{sun} is the hot end's absorbed solar radiation, and Equation2 provides the specific calculation formula:

$$P_{sun} = \cos\varphi \int_{0.25}^{2.5} \varepsilon_h(\lambda,\varphi) I_{sun}(\lambda) d\lambda \;^{[1]} \qquad \text{(Equation 3)}$$

Angle φ for film and vertical angle of the sun's radiation, φ=0° is used in this design. $\varepsilon_h(\lambda,\varphi)$ is the solar absorption at the heat end which controlled by angle and wavelength, $I_{sun}(\lambda)$ for solar spectrum irradiance, this experiment uses 0.25~2.5 µm band explored.[2]

The system receives heat from the environment, which it uses to boost its temperature，

$$P_{atm}(T_{amb}) = \int d\Omega cos\theta \int_{2.5}^{25} d\lambda \varepsilon_h(\lambda.\theta) \varepsilon_{atm}(\lambda,\theta) I_{BB}(\lambda,T_{amb}) \qquad \text{(Equation 4)}$$

Here, Kirchhoff's radiation law was utilized to replace the hot end's absorptivity with its emissivity.[3] The atmospheric emissivity is: $\varepsilon_{atm}(\lambda,\theta) = 1 - t(\lambda)^{1/cos\theta}$, where $t(\lambda)$ is the atmospheric transmission rate of the sky.[2] $\int d\Omega = \int_0^{\pi/2} d\theta \sin\theta \int_0^{2\pi} d\beta$ is the angular integral of a hemisphere. $I_{BB}(\lambda,T) = \frac{2hc^2}{\lambda^5} \frac{1}{e^{hc/\lambda k_B T} - 1}$ is the blackbody's spectral emissivity at temperature T, where h is Planck’s constant, c is the speed of light and l is the wavelength, k_B is the Boltzmann constant. T_{amb} is ambient temperature，T is hot end surface temperature

The heat ends will lose some of its energy due to heat exchange with the surrounding environment, and the formula is

$$P_{cond + conv}(T,T_{amb}) = h_{cc}(T_{atm} - T) \qquad \text{(Equation 5)}$$

$h_{cc} = h_{cond} + h_{conv}$ is the heat transfer coefficient combined convection and conduction. The theoretical maximum energy power is reached when h_{cc} is 0.

3. PSP film Cooling Capacity analysis

The radiative cooling power formula at the cold end is illustrated below.

$$P_{net} = P_{rad}(T) - P_{atm}(T_{amb}) - P_{sun} - P_{cond + conv}(T,T_{amb}) \qquad \text{(Equation 6)}$$

Where the sun's effect differs from the hot end, the particular formula is as follows:

$$P_{sun} = \int_{0.25}^{2.5} \varepsilon(\lambda，\theta_{sun}) I_{AM1.5}(\lambda) d\lambda \qquad \text{(Equation 7)}$$

$I_{AM1.5}(\lambda)$ is the solar illumination, the AM1.5 spectrum, with the irradiance of 893 W·m^{-2}. The structure is believed to have a stable angle to the sky. As a result, the Angle integral is solely determined by Angle θ_{sun}.

The cooling end's radiative cooling power, and the formula is

$$P_{rad}(T)=\int d\Omega cos\theta\int_{2.5}^{25}\varepsilon_h(\lambda,\theta)I_{BB}(\lambda,T)d\lambda \qquad \text{(Equation 8)}$$

4. The equipment of dynamic switching

To simulate the real use of the procedure of testing optical properties, it was inserted in two pieces of glass. Only two circular apertures with a diameter of 3 mm are left as gas/liquid channels at the bottom of the device in this design, and the groove thickness between the two glass plates is 0.6 cm. The liquid flows upwards at 6.3 mL s^{-1}, taking only 15.5 seconds to change the film from opaque to transparent.

$$t=\frac{V}{A\times v}=\frac{V}{\pi\frac{D}{2}^{2}\times v} \qquad \text{(Equation 9)}$$

V is the air gaps between the two cover glasses, A is the area of channels, v is the liquid flow rate, D is the diameter of liquid channels

To transition to the high emission state, all solutions in the groove should always be recycled by gravity through the hose first, then air/nitrogen was fed into at the velocity of 0.33 L s^{-1} flow through a circular opening, and the through-hole liquid and the remaining liquid in the device are blown out or evaporated at an accelerated rate, restoring the film's white luster. As Figure S3 shown.

The power consumption for devices:

In the device hot and cold cycles are carried out by the peristaltic pump and fan, respectively, the peristaltic pump rated power of 20 W, the fan rated power of 16 W, in a cycle process, the peristaltic pump operating time of 15.5 s, the fan operating time of 39 s, so a cycle of the required power is

$$W=P\times t=(20\times15.5\div3600+16\times39\div3600)=0.3\times10^{-3}\ \text{kW·h} \qquad \text{(Equation 10)}$$

W is the amount of power consumed, P is the power and t is the time taken,

The number of times a tent needs to be switched in a day is calculated as three times, then the power consumption required is

$$W=P\times t\times n=(20\times15.5\div3600+16\times39\div3600)\times3=0.9\times10^{-3}\ \text{kW·h} \qquad \text{(Equation 11)}$$

n is the number of times.

EnergyPlus version 9.2 was utilized to predict energy consumption and saving with different boundaries. A model building has three stories, with the building's roof with the size of 2224.52 m^2. Hourly weather data were obtained from https://energyplus.net/.

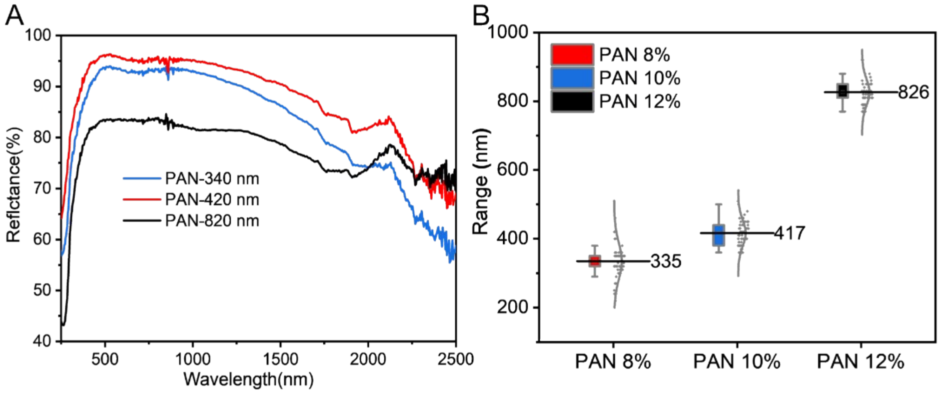

Figure.S1 PAN fiber diameter range and spectrum. (A) Reflectance characteristics of fiber films with different diameters. (B) Fiber diameter distribution under different conditions.

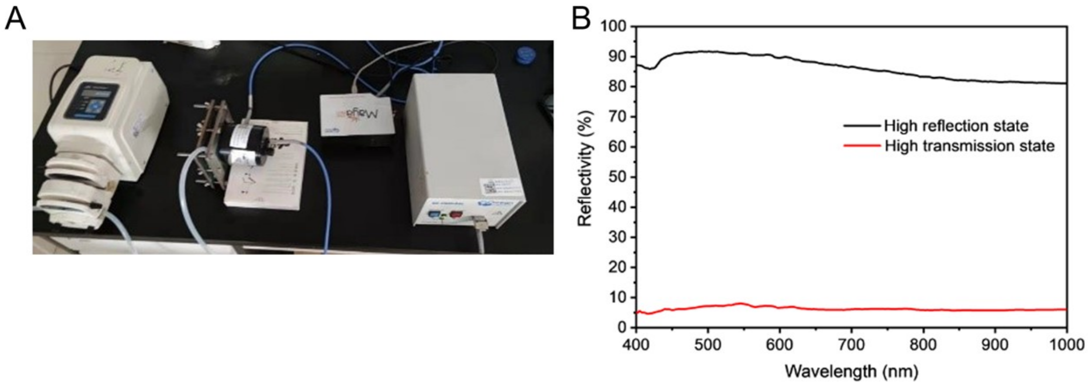

Figure.S2 Spectroscopic response of dynamic switching. (A) Test connection diagram. (B) The high-emission state

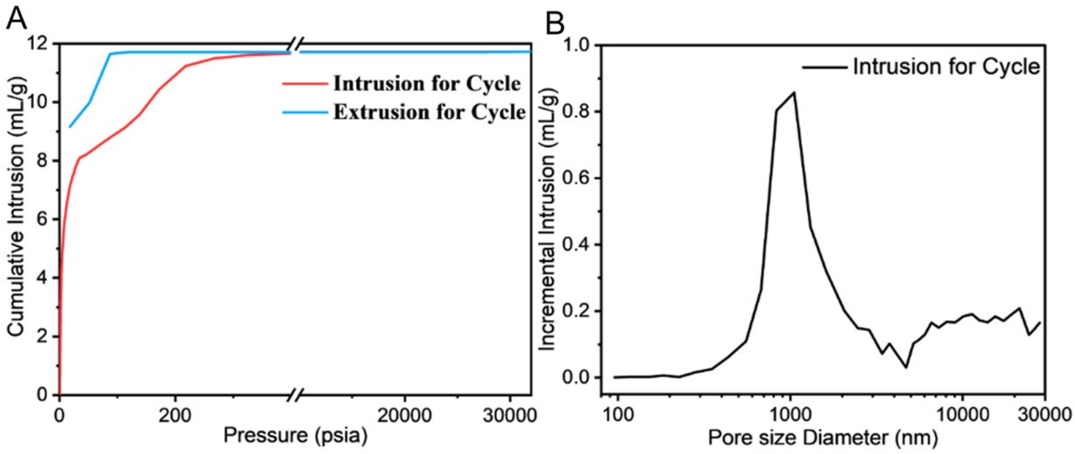

of the PSP film changes to the low-emission state due to the presence of the solution.

Figue.S3 Range of pore sizes for the PSP film. (A) Mercury pressure and mercury removal processes of fiber films. (B) Distribution of pore structure of fiber.

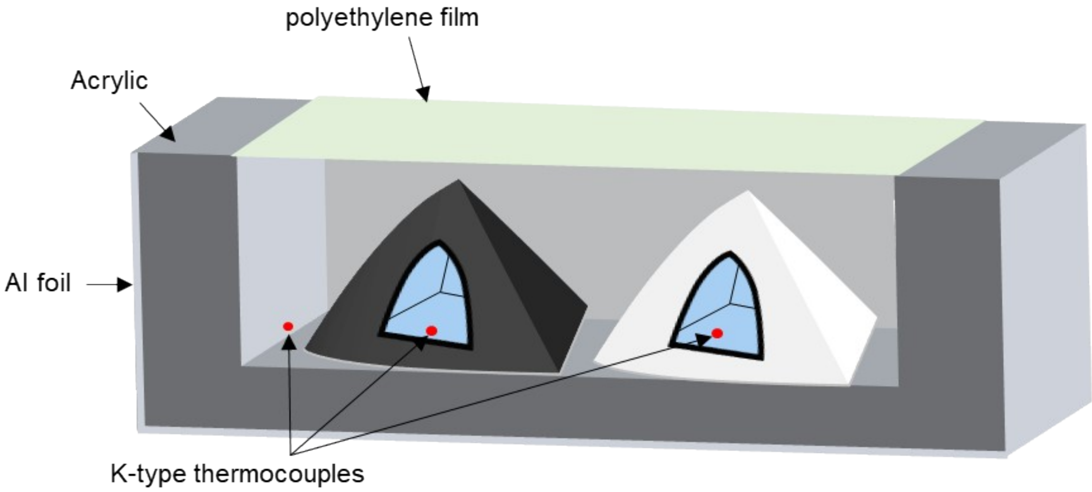

Figure.S4 Schematic of outdoor temperature detection device.

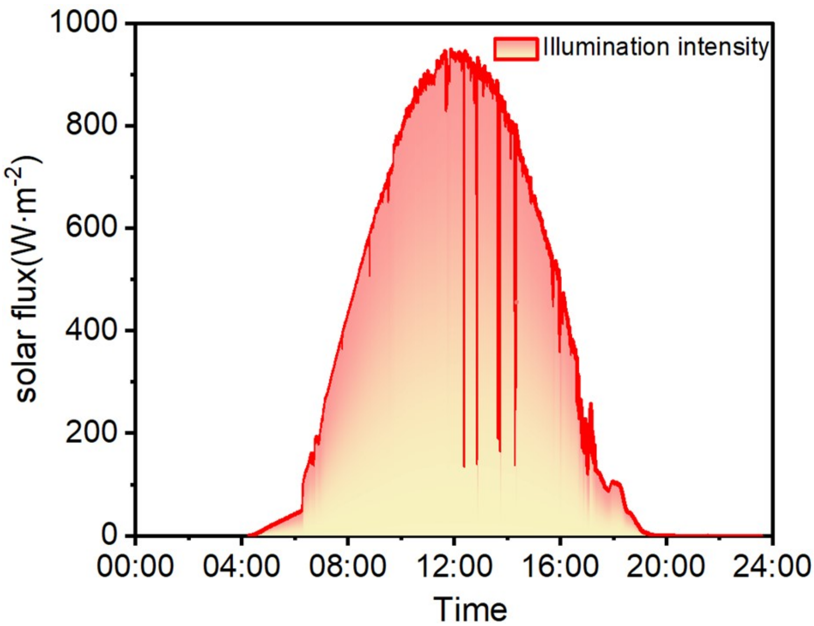

Figure.S5 Depiction the light intensity measured concurrently. Continuous light irradiation intensity was measured simultaneously.

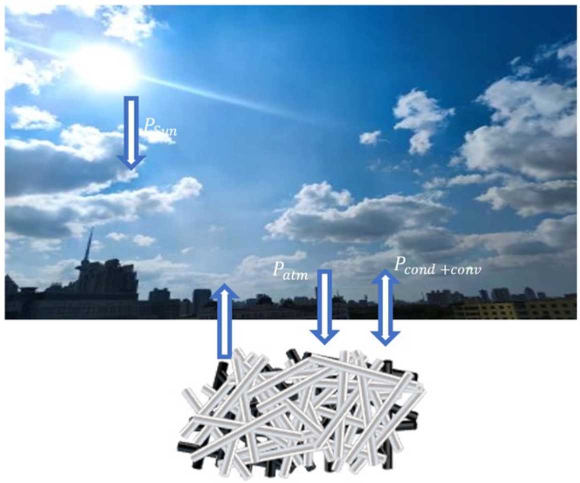

Figure.S6 Heat transfer principles of cooling nanofibers.

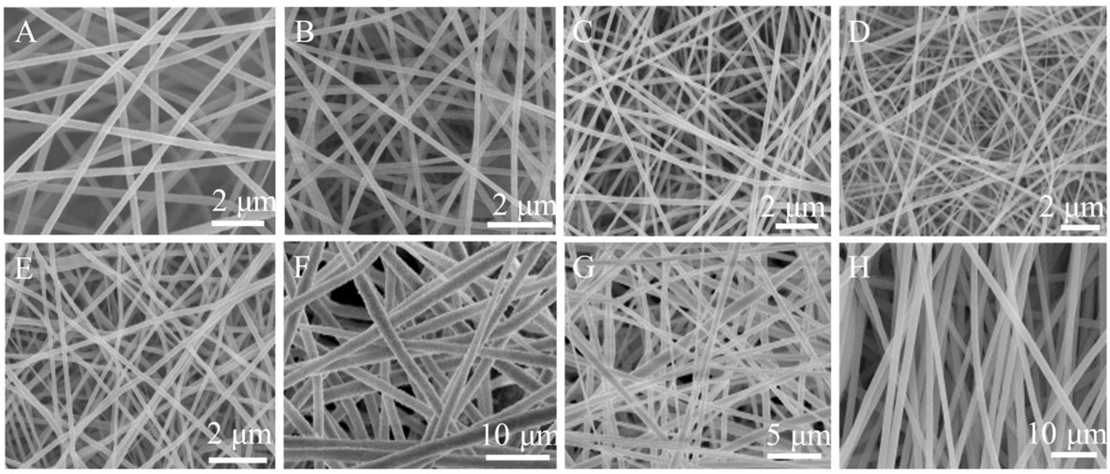

Figure.S7 SEM of different cooling nanofibers. (A-H) PAN, SiO_2, PVA, PSA, PVP, PVDF, PMMA and PS nanofibers.

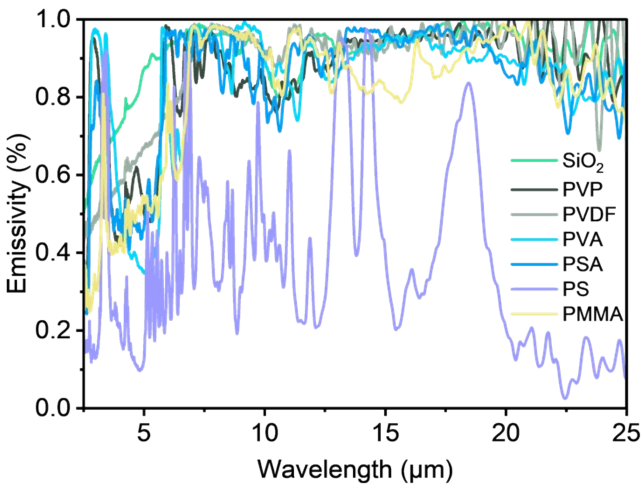

Figure.S8 Infrared emission of nanofibers made of different polymers.

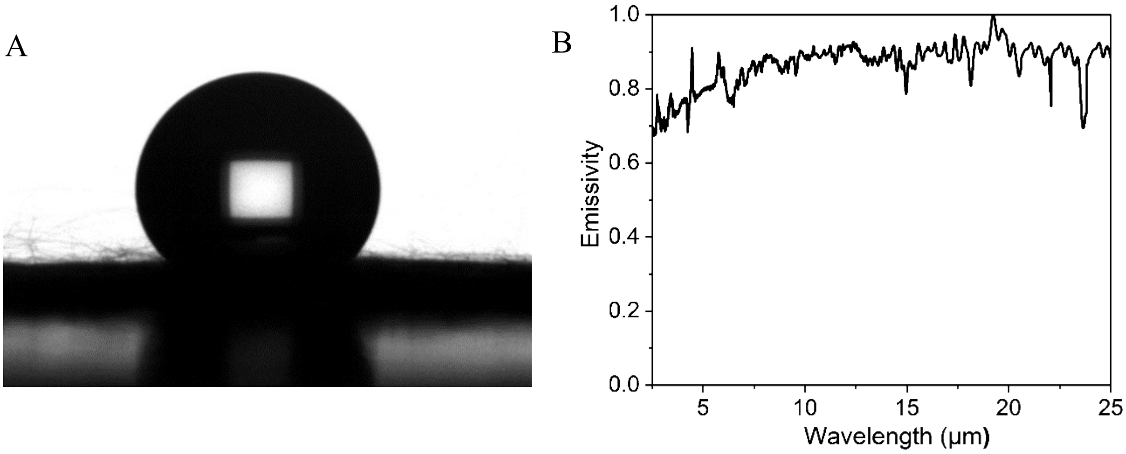

Figure.S9 A.Water contact angle of PSP film. B. The emission performance of the PSP films after simulated rainfall.

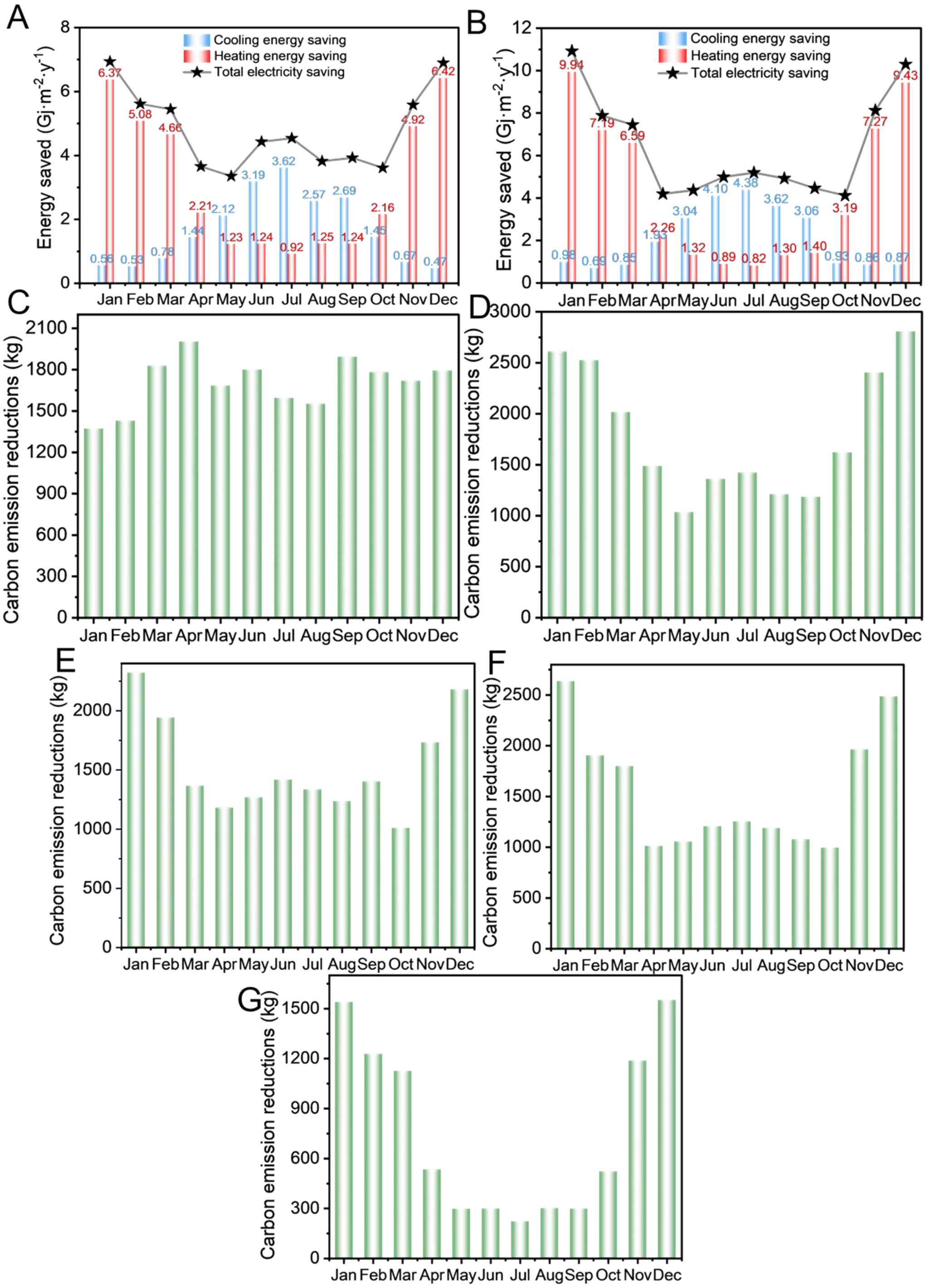

Figure.S10 Energy savings of the PSP films. (A-B) Energy saved in different cities and months in different months. A, B are Lanzhou and Lhasa. C-G are the reduction of CO_2 emissions in Haikou, Harbin, Lanzhou and Lhasa, respectively.

Supplementary Tables

Electrospinning technology can match different materials to prepare membrane materials, including polymers and inorganics. We list the refractive indices of several common substances that can be switched to different solvents, as shown in Table S1.

Table S1. The refractive index of different materials

materials	refractive index	solvent	refractive index
polyvinylidene fluoride	1.42	ethyl alcohol	1.3618
polymethyl methacrylate	1.4893	deionized water	1
polystyrene	1.5894	methyl alcohol	1.3286
polyvinyl alcohol	1.52	isopropyl alcohol	1.3776
polyvinyl pyrrolidone	1.54	glycerin	1.4763
silicon dioxide	1.457	phenethyl alcohol	1.53

Table S2. Details for the comparison with other building thermal control systems.

	Cooling power (W m^{-2})	Heating power (W m^{-2})	Switch mode	Energy saving（GJ y^{-2} m^{-2}）
Ref4 [4]	122	0	Temperature Sense	
Ref5[5]	54.4	0		
Ref6[6]	73	0	mechanical engineering	
Ref7[7]			mechanical engineering	5.21
Ref8[8]	102		mechanical engineering	
Ref9[9]				8.03×10-3
Ref10[10]	71.6	643.4	mechanical engineering	236
Ref11[11]		527	Temperature Sense	
Ref12[12]	93.55	483	Temperature Sense	2.24×10-2
Ref13[13]	26	20.8	mechanical engineering	
Ref14[14]	59.7	252.2	Temperature Sense	1.36
Ref15[15]	126	859.8	mechanical engineering	2.9
This work	111.1	781.6	mechanical engineering	84.97

Movie S1. Dynamic switching of PSP film system. Cold and hot function switches are activated by the solution flowing into and out of the PSP film.

Movie S2. Changes in the radiative cooling film's transmittance.

[1] T. Li, Y. Zhai, S. He, W. Gan, Z. Wei, M. Heidarinejad, D. Dalgo, R. Mi, X. Zhao, J. Song, J. Dai, C. Chen, A. Aili, A. Vellore, A. Martini, R. Yang, J. Srebric, X. Yin, L. Hu, *Science* 2019, **364**, 760.
[2] A. P. Raman, M. A. Anoma, L. Zhu, E. Rephaeli, S. Fan, *Nature.* 2014, 515, 540.
[3] C. G. Granqvist, A. Hjortsberg, *J. Appl. Phys.* 1981, **52**, 4205.
[4] M. Ono, K. Chen, W. Li, S. Fan, *Opt. Express.* 2018, **26**, 777.
[5] B. Zhao, M. Hu, X. Ao, N. Chen, Q. Xuan, D. Jiao, G. Pei, *Appl. Energy.* 2019, **252**, 113432.
[6] J. Mandal, M. Jia, A. Overvig, Y. Fu, E. Che, N. Yu, Y. Yang, *Joule.* 2019, 3, 3088.
[7] J. Liu, Z. Zhou, D. Zhang, S. Jiao, J. Zhang, F. Gao, J. Ling, W. Feng, J. Zuo, *Energy Convers. Manag*. 2020, **205**.
[8] H. Zhao, Q. Sun, J. Zhou, X. Deng, J. Cui, *Adv. Mater.* 2020, **32**, 2000870.
[9] X. Ao, B. Li, B. Zhao, M. Hu, H. Ren, H. Yang, J. Liu, J. Cao, J. Feng, Y. Yang, Z. Qi, L. Li, C. Zou, G. Pei, *Proc. Natl. Acad. Sci. U.S.A.* 2022, **119**, 2120557119.
[10] X. Li, B. Sun, C. Sui, A. Nandi, H. Fang, Y. Peng, G. Tan, P. C. Hsu, *Nat. Commun.* 2020, **11**, 6101.
[11] Z. Xia, Z. Fang, Z. Zhang, K. Shi, Z. Meng, *ACS. Appl. Mater. Interfaces.* 2020, **12**, 27241.
[12] K. Tang, K. Dong, J. Li, M. P. Gordon, F. G. Reichertz, H. Kim, Y. Rho, Q. Wang, C.-Y. Lin, C. P. Grigoropoulos, A. Javey, J. J. Urban, J. Yao, R. Levinson, J. Wu, *Science.* 2021, **374**, 1504.
[13] K. C. S. Ly, X. Liu, X. Song, C. Xiao, P. Wang, H. Zhou, T. Fan, *Adv. Funct. Mater.* 2022, **32**, 2203789.
[14] Q. Zhang, Y. Wang, Y. Lv, S. Yu, R. Ma, *Proc. Natl. Acad. Sci. U.S.A.* 2022, **119**, 2207353119.
[15] Q. Zhang, Y. Lv, Y. Wang, S. Yu, C. Li, R. Ma, Y. Chen, *Nat. Commun.* 2022, **13**, 4874.